# Electronic Supplementary Information

## Selectivity Control for $CO_2$ Electroreduction to Syngas Using $Fe/CuO_x$ Catalysts with High Current Density

*Hui Liu,[a,1] Enting Shi,[a,1] Weiwei Guo,[a,*] Zhaoyang Sun,[a] Zijian Fang,[a] Zhijun Zhu,[a,*] Lei Jiao,[a] Yanling Zhai,[a,*] Xiaoquan Lu[a,*]*

[a] *Institute of Molecular Metrology, College of Chemistry and Chemical Engineering, Qingdao University, Qingdao, 266071, P. R. China.*

[1] *These authors contributed equally to this work.*
**E-mail: guoweiwei21@qdu.edu.cn (W.G.), zhuzhijun@qdu.edu.cn (Z.Z.), zhaiyanling@qdu.edu.cn (Y.Z.), luxq@nwnu.edu.cn (X.L.)*

## Experimental Section

### Materials

Copper sulfate pentahydrate ($CuSO_4 \cdot 5H_2O$, purity>99%), Ferric chloride hydrated ($FeCl_3 \cdot 6H_2O$, purity>99%), Sodium hydroxide (NaOH, purity>99%) were purchased from Alfa Aesar China Co., Ltd. Toray Carbon Paper (CP, TGP-H-60, 19×19 cm) and Nafion N-117 membrane (0.180 mm thick, ≥ 0.90 meg/g exchange capacity) were purchased from Alfa Aesar China Co., Ltd. $CO_2$ (99.999 %) and $N_2$ (99.99 %) were provided by Qingdao Analytical Instrument Company. 1-Butyl-3-methylimidazolium hexafluorophosphate ([Bmim]$PF_6$), 1-butyl-3-methylimidazolium tetrafluoroborat ([Bmim]$BF_4$), 1-butyl-3-methylimidazolium perchlorate ([Bmim]$ClO_4$), 1-butyl-3-methylimidazolium nitratre ([Bmim]$NO_3$) and 1-ethyl-3-methylimidazolium hexafluorophosphate ([Emim]$PF_6$) was purchased from the Centre of Green Chemistry and Catalysis, Lanzhou Institute of Chemical Physics, Chinese Academy of Sciences.

### Catalysts preparation

**Synthesis of Fe/CuO:** We synthesized Fe/CuO used simple Fe-precipitation and calcination method. First, 2.0 g of $CuSO_4 \cdot 5H_2O$ and 0.02 g of $FeCl_3 \cdot 6H_2O$ were dissolved in 100 mL of deionized in a three-neck flask. The three-neck flask was placed in an ice-water bath with vigorous magnetic stirring to form a homogeneous blue solution. Then, 20 mL of NaOH solution (1.2 M) was slowly injected into the flask, and the mixture was continuously stirred for 30 min. After being refrigerated (3 $^oC$) for 24 h, the mixture was transferred into a 50 mL Teflon-lined autoclave, sealed, and heated at 130 $^oC$ for 18 h and then cooled down to room temperature. Finally, the product was filtered after cooling and the precipitate was separated from the solution by centrifugation at 11,000 r.p.m. for 5 min and washed several times with deionized water/ethanol solution and dried in vacuum at 60 $^oC$ overnight. Similarly, the CuO sample was also synthesized following the same procedures but without adding $FeCl_3 \cdot 6H_2O$. Finally, the resulting powder was calcined at 400 $^oC$ for 3 h to obtain Fe/CuO.

**Synthesis of Fe/$CuO_x$:** The Fe/CuO was obtained after cooling to room temperature and then electrochemically reduced at -1.0 V *vs.* $Ag/Ag^+$ for 60 s. The final product can be obtained.

### Catalysts characterization

The actual compositions of Fe in the catalysts was determined by inductively coupled plasma optical emission spectroscopy (ICP-OES, Vista-MPX). X-ray photoelectron spectroscopy (XPS) analysis was performed on the Thermo Scientific ESCALAB Xi+ using 200 W monochromatic Al Kα radiation. The 500 μm X-ray spot was used. The base pressure in the analysis chamber was about $3 \times 10^{-10}$ mbar. X-ray diffraction (XRD) analysis of the samples was performed on the X-ray diffractometer (Rigaku Smartlab SE) with Cu-Kα radiation, and the scan speed was 5° $min^{-1}$. The morphologies of as-synthesized materials were characterized by a FESEM, JEOLJSM-7800F scanning electron microscope (SEM) and a FEI TF20 high-resolution transmission electron microscopy (HR-TEM). $N_2$ adsorption/desorption isotherms of the materials were determined using a Quadrasorb SI-MP system to obtain Brunauer-Emmett-Teller (BET) specific surface area and pore size. The adsorption isotherms of $CO_2$ were determined at 25 $^oC$ in the pressure range of 0-1 atm on a TriStar II 3020 device. The Raman spectra were obtained using a confocal laser micro-Raman spectrometer (Renishaw inVia InSpect confocal Raman microscope, US) with a 585

nm laser. X-ray absorption Near-side Structure (XANES) and Extended X-ray Absorption Fine Structure (EXAFS) tests were performed at the 1W2B beamline at the Beijing Synchrotron Radiation Facility (BSRF), China.

### Electrode preparation

To prepare the Fe/$CuO_x$-CP electrode, 10 mg catalyst was suspended in 1 mL acetone with 20 μL Nafion D-521 dispersion (5 wt%) to form a homogeneous ink. Then, 500 μL of solution was spread onto the CP (1×0.5 $cm^{-2}$) surface by a micropipette and then dried under room temperature. The loading of catalyst was 5.0 mg $cm^{-2}$. Before experiment, all the auxiliary electrodes were sonicated in acetone for 10 min and then washed with water and ethanol, followed by drying in $N_2$ atmosphere.

### Electrocatalytic $CO_2$ reduction

All the electrochemical experiments were conducted on the electrochemical workstation (CHI 6081E). All potentials cited in this work were referenced to the $Ag/Ag^+$. The electrolysis experiments were conducted at 25 °C in a H-type cell with a working cathode, a counter anode (platinum gauze), and a reference electrode $Ag/Ag^+$ (0.01 mol $L^{-1}$ $AgNO_3$ in 0.1 mol $L^{-1}$ TBAP-MeCN). In the experiment, nafion-117 membrane was used as the proton exchange membrane that separated the cathode and anode compartments. MeCN containing 0.5 M [Bmim]$PF_6$ was utilized as cathode electrolyte and 0.5 M $H_2SO_4$ aqueous solution was utilized as anode electrolyte. In each experiment, the amount of electrolyte was 30 mL. Before starting the electrolysis experiment, the catholyte was bubbled with $CO_2$ for 30 min under stirring and the electrolysis was carried out under a steady stream of $CO_2$ (20 sccm).

### Product analysis

The gaseous product of electrochemical experiments was collected using a gas bag and analyzed by gas chromatography (GC, PANNA A60). The liquid product was analyzed by $^1H$ NMR (Bruker Avance III 400 HD spectrometer) in DMSO-$d_6$ with TMS as an internal standard.
The Faraday efficiency of gas products was calculated by the Eq

$$\mathbf{FE} = \frac{\mathbf{n \cdot N_A \cdot e \cdot V \cdot \nu \cdot P / R \cdot T}}{\mathbf{I_{total} \cdot t}} \mathbf{X\ 100\%}$$

(n: transfer electron number; $N_A$: Avogadro constant; $\nu$: gas-flow rate; P: standard atmospheric pressure; R: gas constant; T: temperature; I: total current; t: reaction time)

### Tafel analysis

The partial current densities for products under different potentials were measured. The overpotential was obtained from the difference between the equilibrium potential and the catalytic potential. Multiple electrolysis experiments were performed at each potential to obtain the current density versus overpotential data in the H-type electrolysis cell as described above. Tafel plots were constructed from these data.

### Electrochemical surface areas (ECSAs) study

The cyclic voltammetry measurement was conducted in MeCN containing 0.5 M [Bmim]$PF_6$

solution using a three-electrode system at 25 ºC. Cyclic voltammogram measurements of the five catalysts were conducted from -1.59 to -1.69 V vs $Ag/Ag^+$ with various scan rates to obtain the double layer capacitance (*C*dl) of $Fe/CuO_x$ catalyst. The *C*dl was estimated by plotting the $\Delta j$ ($ja$-$jc$) at -1.64 V vs $Ag/Ag^+$ against the square root of scan rates, in which $ja$ and $jc$ were the anodic and cathodic current density, respectively.

**Electrochemical impedance spectroscopy (EIS) study**

The experimental apparatus was the same as that for LSV measurements. The EIS measurement was carried out in MeCN containing 0.5 M $[Bmim]PF_6$ aqueous solution at an open circuit potential (OCP). The data obtained from the EIS measurements were fitted by the software of Zview (Version 3.1,Scribner Associates, USA).

**Supplementary Figures**

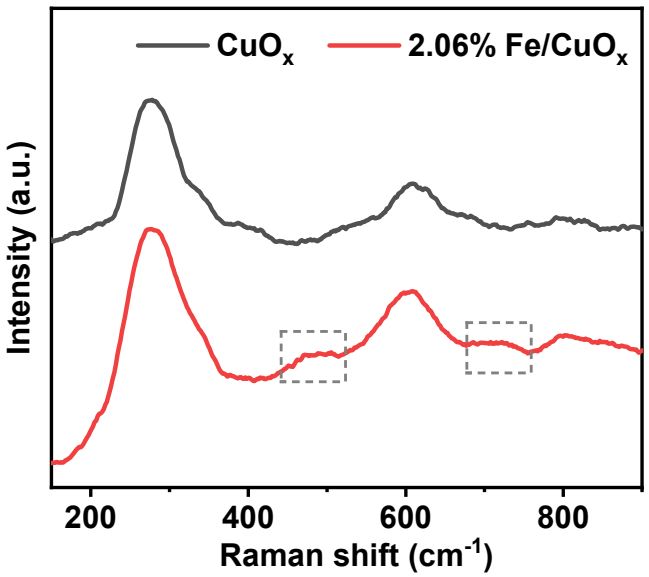


**Fig S1** The Raman spectra of 2.06%Fe/$CuO_x$ and $CuO_x$ in the range of 200-800 $cm^{-1}$.

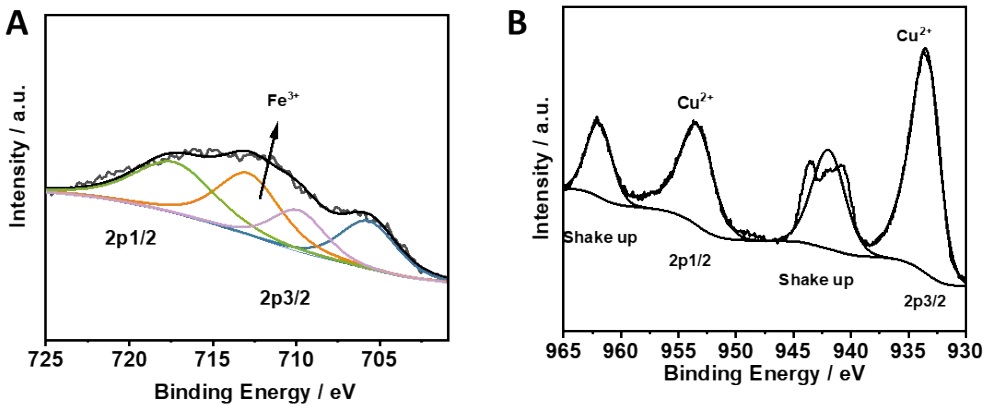


**Fig. S2** XPS spectra of Fe 2p (A) and Cu 2p (B) orbits of 2.06%Fe/$CuO_x$.

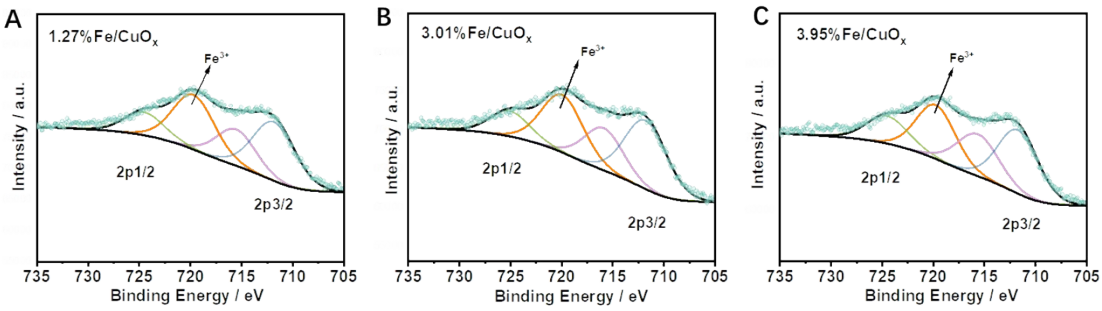


**Fig. S3** XPS spectra of Fe 2p orbits of A) 1.27%Fe/$CuO_x$, B) 3.01%Fe/$CuO_x$, C) 3.95%Fe/$CuO_x$.

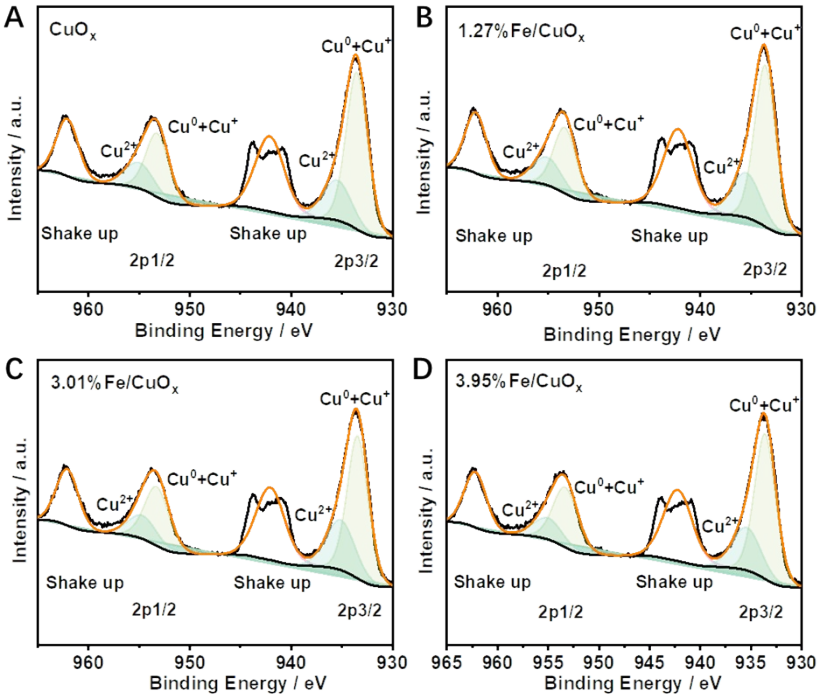


**Fig. S4** XPS spectra of Cu 2p orbits of A) $CuO_x$, B) 1.27%Fe/$CuO_x$, C) 3.01%Fe/$CuO_x$, D) 3.95%Fe/$CuO_x$.

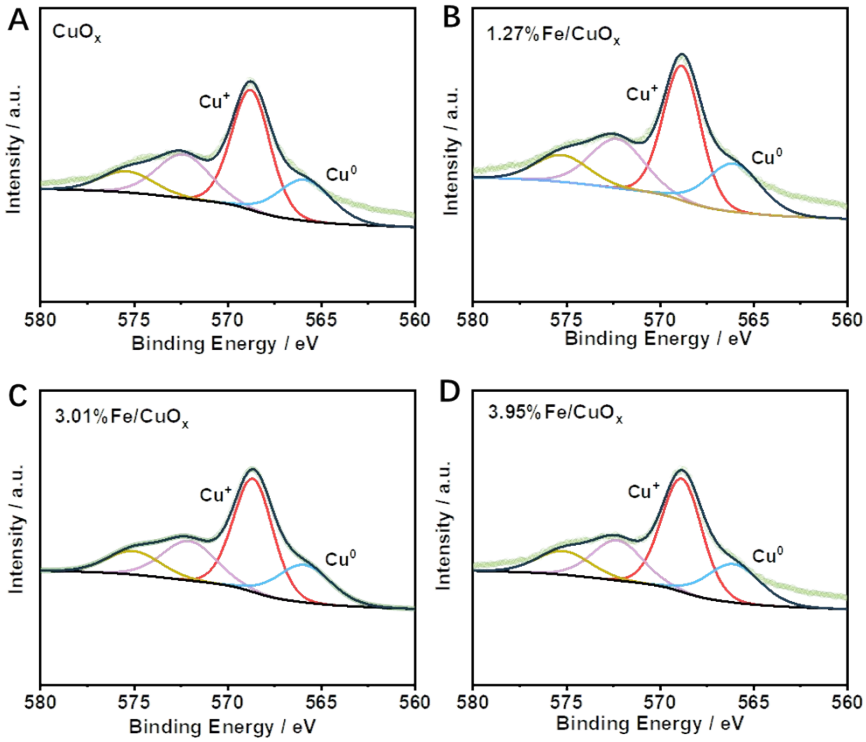


**Fig. S5** AES spectrum of Cu LMM for of A) $CuO_x$, B) 1.27%Fe/$CuO_x$, C) 3.01%Fe/$CuO_x$, D) 3.95%Fe/$CuO_x$.

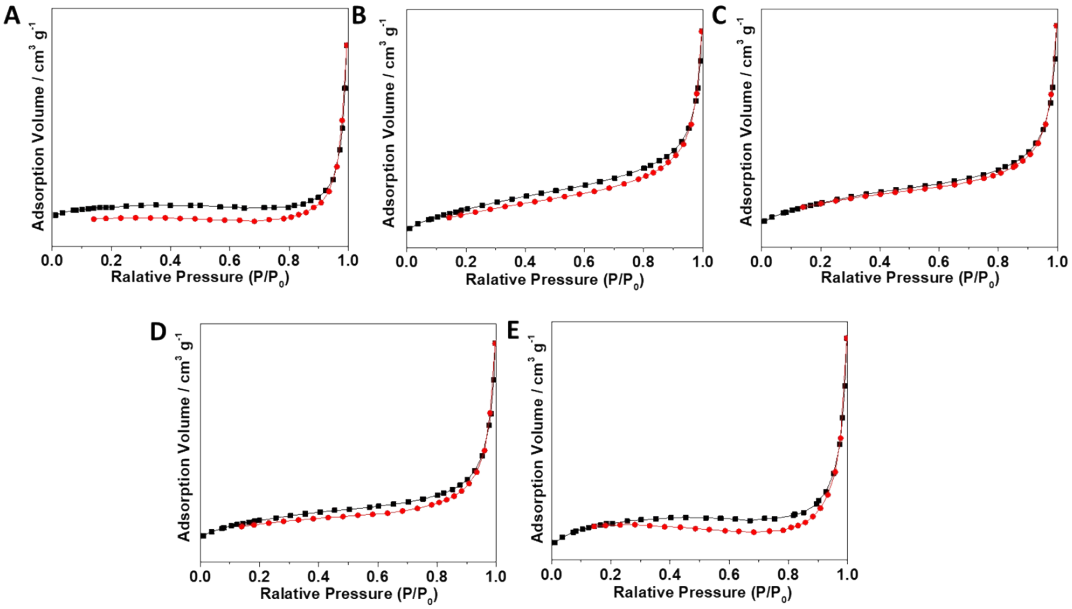


**Fig. S6** $N_2$ adsorption/desorption isotherms of A) $CuO_x$, B) 1.27%Fe/$CuO_x$, C) 2.06%Fe/$CuO_x$, D) 3.01%Fe/$CuO_x$, and E) 3.95%Fe/$CuO_x$. The surface areas of different catalysts were calculated to be 5.6, 9.7, 11.3, 8.9 and 7.2 $m^2$ $g^{-1}$ using the Brunauer–Emmett–Teller (BET) model, respectively.

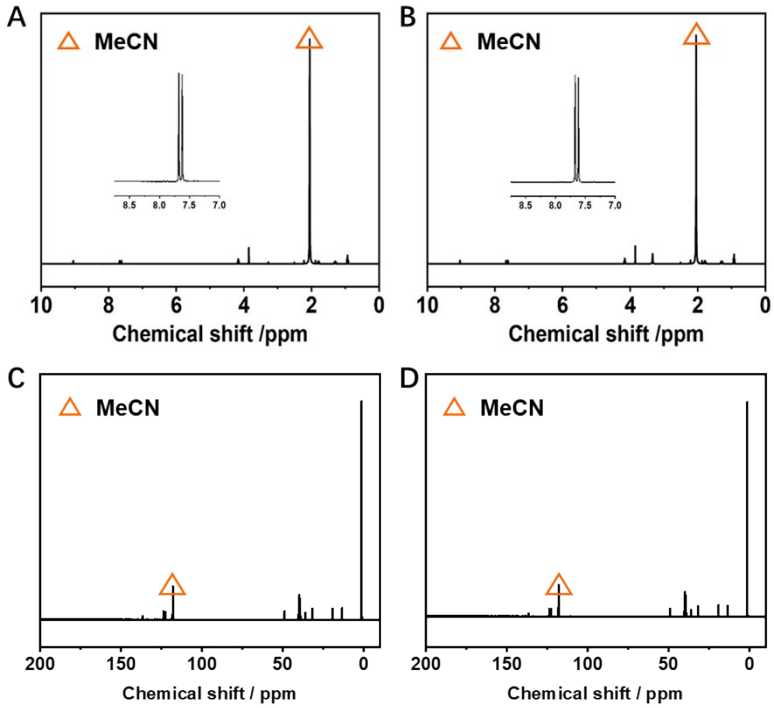


**Fig. S7** $^{1}$H-NMR spectra of 0.5 M [Bmim]$PF_6$/MeCN before A) and after B) electrolysis on 2.06%Fe/$CuO_x$, $^{13}$C-NMR spectra of 0.5 M [Bmim]$PF_6$/MeCN before C) and after D) electrolysis on 2.06%Fe/$CuO_x$, the applied potential is -2.1V *vs.* $Ag/Ag^+$ (DMSO-$d_6$).

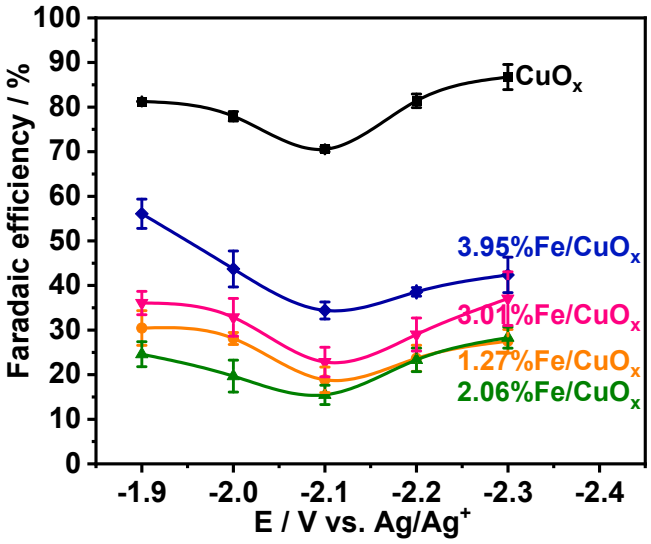


**Fig. S8** Faradaic efficiency of $H_2$ for different catalysts at the applied potentials.

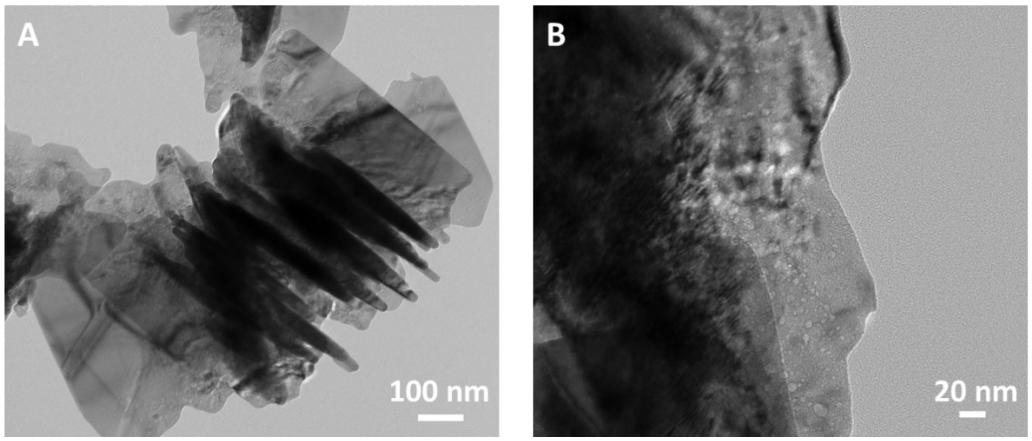


**Fig. S9** TEM image of 3.95%Fe/$CuO_x$.

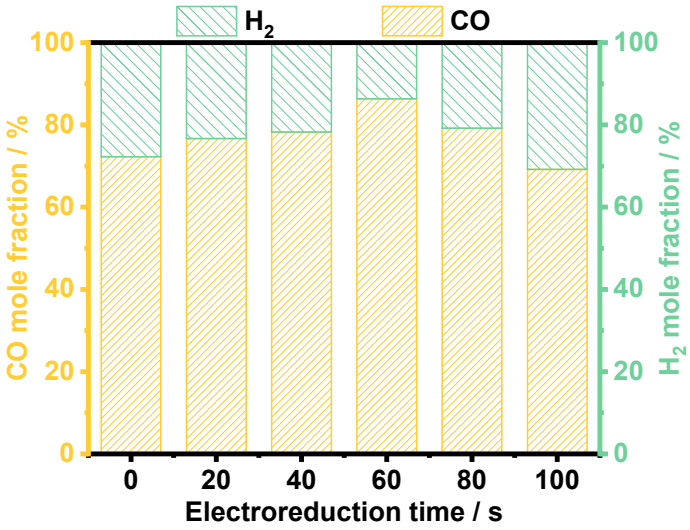


**Fig. S10** CO and $H_2$ mole fraction over 2.06%Fe/$CuO_x$ catalyst by different reduction times at −2.1 V *vs.* $Ag/Ag^+$.

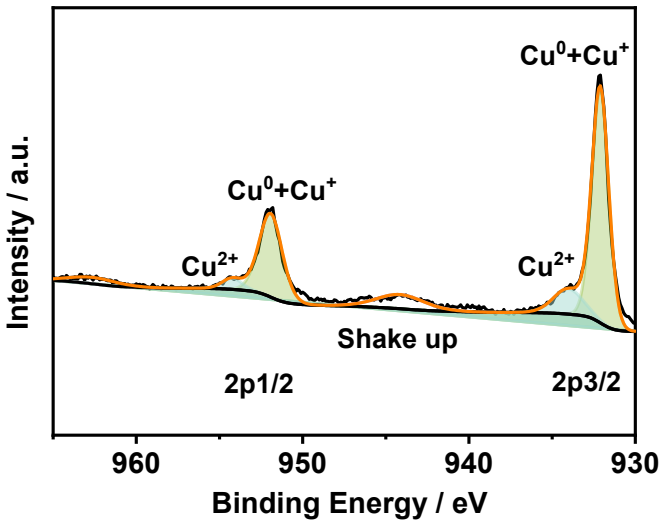


**Fig. S11** XPS spectra of Cu 2p orbits of 2.06%Fe/$CuO_x$ catalyst after 300 s electroreduction.

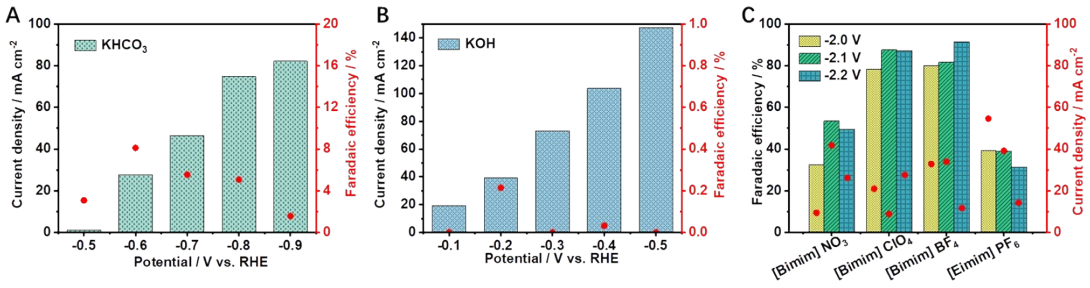


**Fig. S12** Total current density and the FE(CO) of 2.06%Fe/$CuO_x$ at the applied potentials in A) 0.5 M $KHCO_3$ aqueous solution, B) 1.0 M KOH aqueous solution and C) different ionic liquid-based electrolytes.

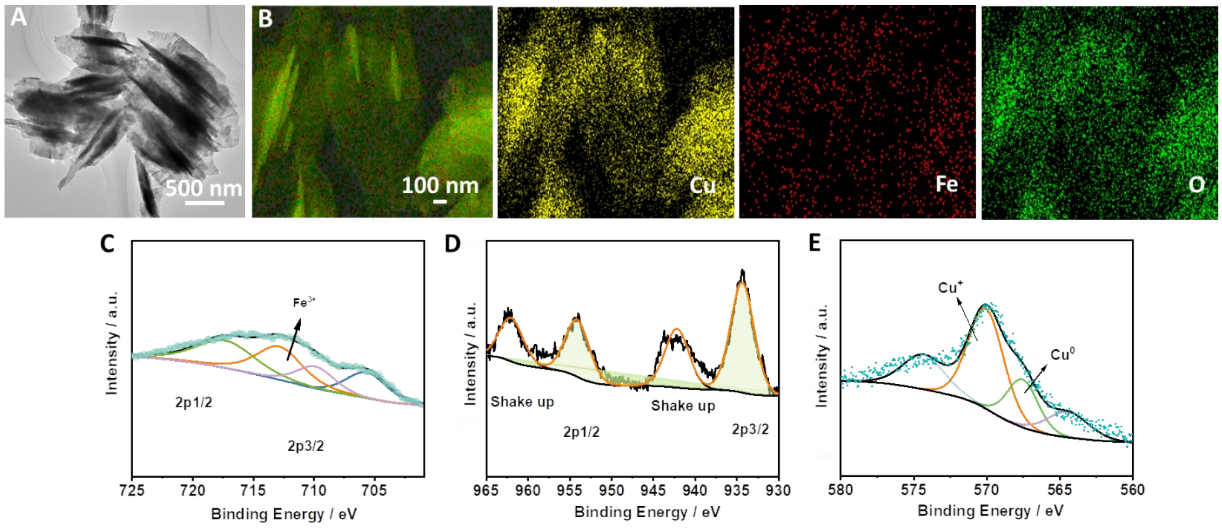


**Fig. S13** A) TEM image, elemental B) mappings and merged images of 2.06%Fe/$CuO_x$ after electrolysis for 2 h. XPS spectra of the catalyst: high resolution spectra of Fe 2p C) and Cu 2p D) of 2.06%Fe/$CuO_x$ after electrolysis. E) AES spectrum of Cu LMM after electrolysis.

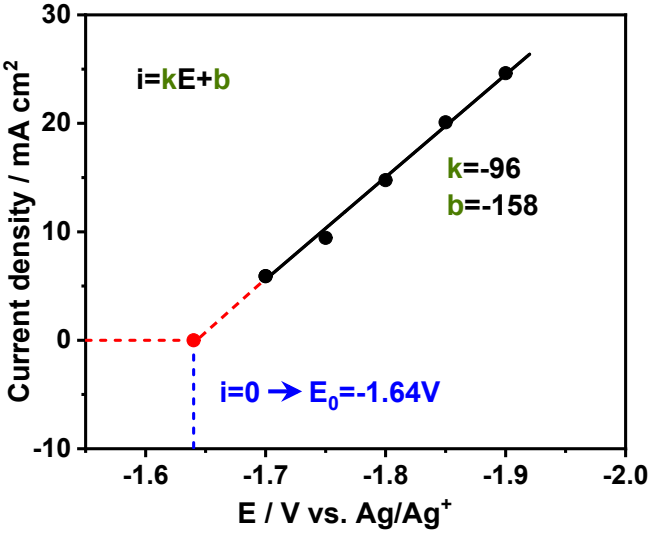


**Fig. S14** The extrapolation method of calculating equilibrium potential.

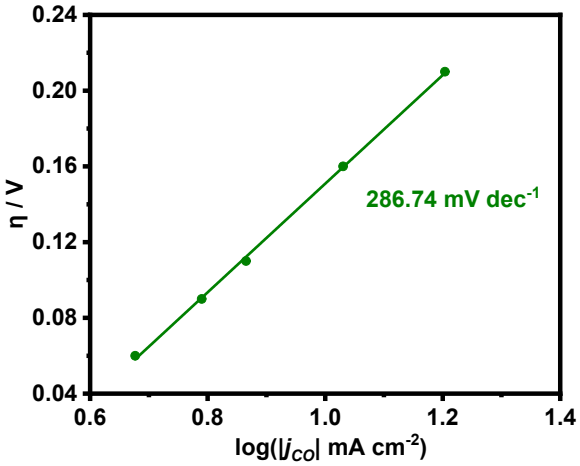


**Fig. S15** Tafel plot for CO production over 2.06%Fe/$CuO_x$.

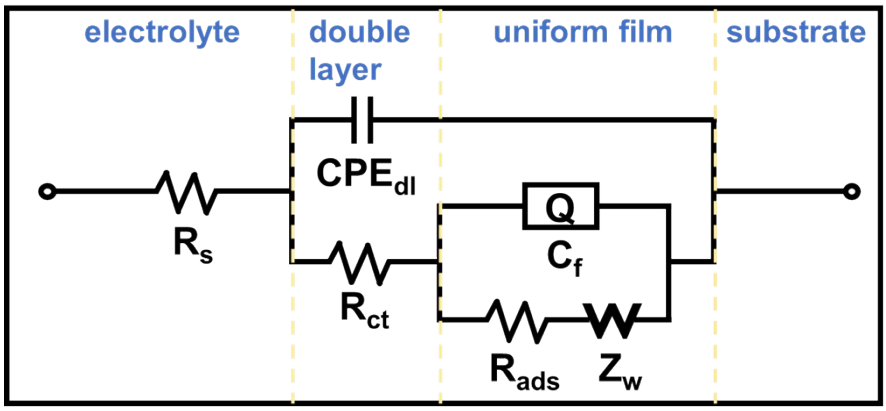


**Fig. S16** Electrical equivalent circuit used for simulating the experimental impedance data.

## Supplementary Tables

**Table S1** The ICP results of different catalysts.

| Sample | Fe / wt% |
|---|---|
| $CuO_x$ | 0 |
| 1.27%Fe/ $CuO_x$ | 1.27 |
| 2.06%Fe/ $CuO_x$ | 2.06 |
| 3.01%Fe/ $CuO_x$ | 3.01 |
| 3.95%Fe/ $CuO_x$ | 3.95 |

**Table S2.** Literature reviews of $CO_2$ electroreduction to syngas using different catalysts.

| Catalysts | Range of $CO/H_2$ | Maximum $FE_{CO}$ (%) | $j_{CO}$ (mA $cm^{-2}$) | Reference |
|---|---|---|---|---|
| $Fe/CuO_x$ | 1.94-6.18 | 86.1 | 42.2 | This work |
| Pd/C | 0.5-1 | ~50 | ~0.3 | S1 |
| Au/TiNS | 0.03-4 | 81.9 | ~10 | S2 |
| silver nanowires | 1-4 | 80 | ~6 | S3 |
| $Ag/C_3N_4$ | 2-100 | 99 | ~10 | S4 |
| Cu−In alloys | 0.06-0.38 | ~30 | ~2.3 | S5 |
| MoSeS alloy monolayers | ~1 | 45.2 | 43 | S6 |
| $Co_3O_4$-Cdots-$C_3N_4$ | 0.07-4 | 89 | 15 | S7 |
| $MoS_2$ | 0.5-4 | 81.2 | - | S8 |
| Zn | 0.25-2.31 | 85 | ~10 | S9 |
| Fe-N-C | 0-4 | 90 | 6 | S10 |
| F-γ-$In_2Se_3$/CP | 0.33-24 | 96.5 | 55.3 | S11 |
| CoNi-NC Single-Atom | 0.23-2.26 | 45~55 | ~35 | S12 |
| $AgP_2$ | 0.33-5 | 82 | 8.7 | S13 |
| $ZnO-Ni_x$ | 0.1-4.5 | ~68 | ~3.6 | S14 |
| nh-CuIn | 0.5-2.13 | 71.4 | 5.5 | S15 |
| Ni-N-GA | 0.4-2.5 | 74 | - | S16 |
| Fe@NBCT | 0.14-4 | 82.7 | ~8 | S17 |
| Te-Pd $NP_s$/C | 0.27-5.37 | 83.7 | - | S18 |
| Co-N-C-Ph | 0.83-1.5 | 60 | ~6 | S19 |
| $Au_{25}(SR)_{18}$ $PtAu_{24}(SR)_{18}$ | 0.25-1 | ~95 | 12 | S20 |
| CoNi-NC | 0.23-2.26 | 55 | ~36 | S21 |

## References


1 W. Sheng, S. Kattel, S. Yao, B. Yan, Z. Liang, C. J. Hawxhurst, Q. Wu, J. G. Chen, *Energy Environ. Sci.,* 2017, **10**, 1180.

2 F. Marques Mota, D. L. T. Nguyen, J.-E. Lee, H. Piao, J.-H. Choy, Y. J. Hwang, D. H. Kim, *ACS Catal.,* 2018, **8**, 4364.

3 W. Xi, R. Ma, H. Wang, Z. Gao, W. Zhang, Y. Zhao, *ACS Sustain. Chem. Eng.*, 2018, **6**, 7687.

4 K. Lv, C. Teng, M. Shi, Y. Yuan, Y. Zhu, J. Wang, Z. Kong, X. Lu, Y. Zhu, *Adv. Funct. Mater.*, 2018, **28**, 1802339.

5 Z. B. Hoffman, T. S. Gray, K. B. Moraveck, T. B. Gunnoe, G. Zangari, *ACS Catal.,* 2017, *7*, 5381.

6 J. Xu, X. Li, W. Liu, Y. Sun, Z. Ju, T. Yao, C. Wang, H. Ju, J. Zhu, S. Wei, *Angew. Chem. Int. Ed.,* 2017, **56**, 9121.

7 S. Hernandez, M. A. Farkhondehfal, F. Sastre, M. Makkee, G. Saracco, N. Russo, *Green Chem.,* 2017, **19**, 2326.

8 S. Guo, S. Zhao, X. Wu, H. Li, Y. Zhou, C. Zhu, N. Yang, X. Jiang, J. Gao, L. Bai, *Nat. Commun.*, 2017, **8**, 1828.

9 B. Qin, Y. Li, H. Fu, H. Wang, S. Chen, Z. Liu, F. Peng, *ACS Appl. Mater. Interfaces,* 2018, **10**, 20530.

10 T. N. Huan, N. Ranjbar, G. Rousse, M. Sougrati, A. Zitolo, V. Mougel, F. Jaouen, M. Fontecave, *ACS Catal.*, 2017, **7**, 1520.

11 D. Yang, Q. Zhu, X. Sun, C. Chen, W. Guo, G. Yang and B. Han, *Angew. Chem. Int. Ed.*, 2019, **58**, 1.

12 Q. He, D. Liu, J. H. Lee, Y. Liu, Z. Xie, S. Hwang, S. Kattel, L. Song and J. G. Chen, *Angew. Chem. Int. Ed*., 2020, **59**, 3033.

13 H. Li, P. Wen, D. S. Itanze, Z. D. Hood, X. Ma, M.Kim, S. Adhikari, C. Lu, C. Dun, M. Chi, Y. Qiu and S. M. Geyer, *Nat. Commun.*, 2019, **10**, 5724.

14 J. Wang, Q. Xiang, W. Zhang, F. Shi, F. Li, P. Tao, C. Song, W. Shang, T. Deng and J. Wu, *ACS Appl. Energy Mater*., 2022, **5**, 5531.

15 X. Ma, F. Wang, D. Jiao, D. Zhang, X. Zhao, D. J. Singh, J. Zhao, X Cui and W. Zheng, *Sci. China Mater.*, 2022, **65**, 3504.

16 D. Ping, S. Huang, S. Wu, Y. Zhang, F. Yi, L. Han, S. Wang, H. Wang, X. Yang, D. Guo, J. Hao, S. Fang, *Int. J. Hydrogen Energy.*, 2022, **47**, 23653.

17 R. Yun, B. Zhang, F. Zhan, Z Xin, T. Sheng and Z. Shi, *Inorg. Chem.*, 2022, **61**, 9375.

18 K. Cao, Y. Ji, S. Bai, X. Huang, Y. Li and Q. Shao, *J. Mater. Chem. A*, 2021, **9**, 18349.

19 Z. Guo, Q. Zhang, F. Shen, H. Liu, H. Zhang, Z. Guo, B. Jin, R. Peng, *Electrochim. Acta.*, 2021, **388**, 138647.

20 W.Choi, H. Seong, V. Efremov, Y. Lee, S. Im, D. H. Lim, J. S. Yoo and D. Lee, *J. Chem. Phys.*, 2021, **155**, 014305.

21 Q. He, D. Liu, J. H. Lee, Y. Liu, Z. Xie, S. Hwang, S. Kattel, L. Song and J. G. Chen, *Angew. Chem. Int. Ed.*, 2020, **59**, 3033.